Phys. Status Solidi C **7**, No. 2, 145–148 (2010) / **DOI** 10.1002/pssc.200982456

physica status solidi c
www.pss-c.com
current topics in solid state physics

Ab initio investigation of the $LiNbO_3$ (0001) surface

Simone Sanna[*,1], Alexander V. Gavrilenko[2], and Wolf Gero Schmidt[1]

[1] Lehrstuhl für Theoretische Physik, Universität Paderborn, 33095 Paderborn, Germany
[2] Norfolk State University, Center for Materials Research, VA 23504 Norfolk, USA

Received 4 July 2009, revised 21 September 2009, accepted 14 October 2009
Published online 3 December 2009

PACS 05.70.Np, 68.35.Md, 68.47.Gh, 77.84.Dy, 82.65.+r

[*] Corresponding author: e-mail sanna@phys.upb.de, Phone: +49-5251-602324, Fax: +49-5251-603435

The polar surfaces of ferroelectric $LiNbO_3$ have been investigated by an *ab initio* thermodynamical approach. Basing on density functional theory total energy calculations, we discuss the relative stability of a series of candidate surface structures with varying stoichiometry and surface reconstruction in dependence on the chemical environment. We determine the equilibrium geometry for the positively and negatively polarised surfaces and then discuss the influence of different stabilising mechanisms on the preferred terminations. Positive and negative surfaces are found to have different structure, stoichiometry and ionisation energy. The positive surface is found to contain more oxygen than the negative surface at similar conditions. Different stabilisation mechanisms like stoichiometry modification and reconstruction contribute to stabilise the polar surfaces.

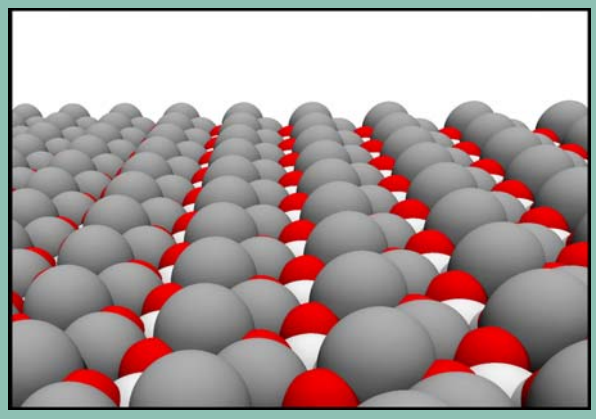

Space-fill model of the reconstructed $LiNbO_3$ (0001) positive surface. White atoms are Nb, gray atoms Li and small gray atoms O.

1 Introduction Lithium niobate ($LiNbO_3$, LN) is a human-made dielectric material which does not exist in nature. Its unusual and favourable optical, piezoelectric, pyroelectric, electro-optic, elastic, photoelastic and photorefractive properties make LN one of the most used materials for acoustic and opto-electronic applications [1]. While traditional applications mainly exploit LN bulk properties, more recently the surfaces and interfaces have become important [2,3]. Periodically poled structures of LN [4] and substrate assisted self-assembly of nanostructures [5] are examples of the emerging applications which require the precise control of ferroelectric domains. Detailed knowledge of the polarisation and charge distribution of the surface is necessary to control the local electronic structure and chemical reactivity. Unfortunately, only few experimental [6–8] and theoretical studies [9] of the LN (0001) surface have been reported in the literature, not least because of the difficulties related to the investigation of the system. LN is a complex bimetallic oxide with spontaneous ferroelectric polarisation directed along the [0001] direction. Cutting the material perpendicularly to this direction will result in the creation of two differently polarised (0001) surfaces, which show peculiar properties like macroscopic polarisation charge. Surface polarisation charges are usually screened by the formation of a compensating charge-layer (internal screening) and by the adsorption of charged molecules (external screening). Moreover, other stabilization mechanisms like surface reconstruction and changes in the surface stoichiometry and electronic structure may contribute to lower the surface energy. Thus, the physical and chemical surface properties of ferroelectrics like LN are controlled by the direction of the

spontaneous polarisation and by the stabilisation mechanisms [10, 11]. Furthermore, the surface structure and stoichiometry will strongly depend on the growth conditions (temperature and constituents partial pressures) of the material. The subtle balance between the ionic and covalent character of the metal-oxygen bonds can in fact be affected by the smallest temperature changes during the growth, resulting in an inversion of the polarisation direction [12].

To determine the electronic and structural characteristics of the LN (0001) surfaces and better understand the stabilisation mechanisms, we investigate the relative thermodynamical stability of different candidate structures with varying stoichiometry and surface reconstruction in dependence on the chemical environment. We find that both a change of the surface structure and stoichiometry contribute to reach an energetically stable state and that the spontaneous polarisation direction strongly influences the surface stoichiometry.

2 Methods The density functional theory (DFT) within the generalised gradient approximation (GGA) as implemented in the VASP simulation packages [13] has been used to simulate the bulk phases of LN, Li_2O, Nb_2O_5, Li and Nb, the oxygen dimer and the LN slabs modelling the different surfaces. This approach was recently shown to yield reliable structures and energies for bulk LN both in its paraelectric and ferroelectric phase [14].

2.1 Computational The total energies of the investigated bulk phases have been calculated using in each case the primitive cell and a converged Monkhorst-Pack [15] k-points mesh. The DFT-GGA approach overestimates the binding energy of the oxygen dimer. We do not correct for this overestimation, as the correction would not qualitatively change any of the conclusions we come to in this work. Ferroelectric LN can be considered a stapling of Nb-O_3-Li trilayers along the [0001] axis. The slabs for the simulation of ferroelectric LN (0001) surfaces are hexagonal supercells consisting of 12 Nb-O_3-Li trilayers (60 atoms) plus a surface termination and a vacuum layer of $\approx$ 15 Å. Following the approach described in Ref. [9] we consider -Nb-O_x-Li_y as positive termination and -O_i-Li_j as negative surface termination, whereby x =1, 2, 3, 4, y =0, 1, 2, i =0, 1, 2, 3, j =0, 1. All the possible combinations have been simulated. Considering the different starting geometries of each termination more than 80 surfaces have been investigated. The outer three trilayers (i.e. 9 LN layers) and all the terminations atoms are allowed to relax in all directions (force threshold 0.02 eV $Å^{-1}$), while the remaining layers are kept fixed to simulate the bulk of the material. The dipole correction described in [16, 17] has been used to correct the artificial forces created by the slab images. This allows the estimation of the ionisation energy for asymmetric slabs. We do not consider other slabs than the 1×1 surface unit cell. A Γ-centred $2 \times 2 \times 1$ k-point mesh was used to carry out the integration in the Brillouin zone, the energy cutoff for the plane wave basis was 400 eV.

2.2 Thermodynamic approach and chemical potentials We adopt the approach described in Ref. [11] to discuss the relative stability of surfaces with different stoichiometry at different growth conditions. The growth conditions are represented by the chemical potentials of Li, Nb and O, which are, on turn, linearly dependent and constrained by the stability of the various phases. Calling μ_{Li}, μ_{Nb} and μ_{O} the deviations of the chemical potentials of Li, Nb and O from their bulk values, the relationships between them are given by:

$$\mu_{\mathrm{Li}} + \mu_{\mathrm{Nb}} + 3\mu_{\mathrm{O}} = -\Delta H_f^{\mathrm{LN}} \tag{1}$$

$$2\mu_{\mathrm{Li}} + \mu_{\mathrm{O}} = -\Delta H_f^{\mathrm{Li_2O}} \tag{2}$$

$$2\mu_{\mathrm{Nb}} + 5\mu_{\mathrm{O}} = -\Delta H_f^{\mathrm{Nb_2O5}} \tag{3}$$

where ΔH_f^i is the formation enthalpy of the compound i. These stability criteria can be brought together in the chemical potential map shown in Fig. 1. At any point within the triangle ADG the sum of μ_{Li}, μ_{Nb} and μ_{O} yields to the formation enthalpy of LN (Eq. (1)). The region enclosed within the points B, D and F satisfies Eq. (2), while the region enclosed between the points A, C, E and G satisfies Eq. (3). The intersection of these regions (the shaded region in Fig. 1) is the thermodynamically allowable range of chemical potentials [18]. Values of the chemical potentials outside this region will not lead to the formation of LN surfaces but to the precipitation of other condensed phases on the LN surfaces.

3 Results As the chemical potentials are not independent, one of them can be expressed in function of the other two. We chose to express μ_{Nb} as function of μ_{Li} and μ_{O}, as the latter can be better controlled during the growth or in experiments. Furthermore, with this choice our results are directly comparable with the data present in the literature [9]. The calculated phase diagrams of the positive and negative LN (0001) surfaces in dependence on μ_{Li} and μ_{O} are shown in Fig. 2. The outlined area denotes the thermodynamically allowed region. It is evident that positive and negative surfaces have quite different stoichiometries, showing that the intrinsic polarisation plays an important role in the surface stabilisation.

The dominating termination for the positive surface is -Nb-O_3-Li_2, while for the negative surface the O-Li- termination is favoured under most condition. Under O-rich conditions the surface can become O_2- or O_3- terminated. In general, the terminations of the positive surface contain more oxygen than these of the negative surface under the same conditions.

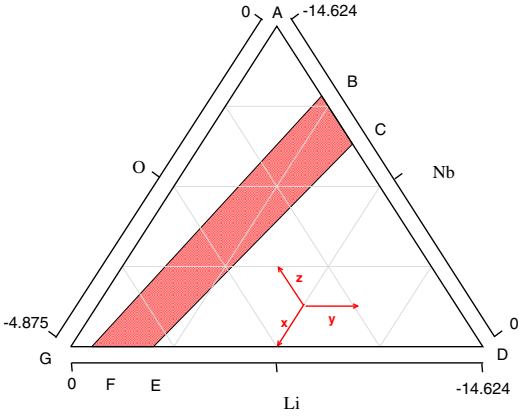

Figure 1 Stability range of the chemical potentials of the $LiNbO_3$ constituents. The region enclosed between B, D, and F satisfies Eq. (2), while the region enclosed between the points A, C, E and G satisfies Eq. (3). The shaded region is the intersection between them and represents the thermodynamically allowed range of the chemical potentials. All the values in eV.

The relaxed atomic structure of the preferred terminations for the positive and negative surface are shown in Fig. 3. While the negative surface does not show any change in the succession of the atomic planes stapled along the [0001] direction with respect to the bulk, the positive surface is characterised by the relaxation of one Li into the lower laying oxygen plane.

4 Discussion After determining the preferred terminations it remains to explain how they stabilise the positive and negative LN (0001) surface. In an attempt to identify the dominant stabilisation mechanism (electronic passivation, stoichiometry changes, reconstruction), we have calculated the ionisation energy for the unrelaxed terminations (W_{ideal}), the ionisation energy for the relaxed terminations (W_{relaxed}) and the surface dipole $\Delta\Phi_{\mathrm{dipole}}$, as described in [19] and in [20] respectively. Let us concentrate for a while on the positive surface. An analysis of the surface band structure shows the metallic nature of the stable -Nb-O_3-Li_2 termination, which means that the electronic passivation of the surface cannot be the main driving force for surface stabilisation at the LN (0001). The values of the ionisation energy of the investigated terminations of the positive surface (without the relaxation effects) are reported in the second column of Tab. 1. Of all the investigated stoichiometries, the -Nb-O_3-Li_2 termination is the more efficient in reducing the ionisation energy W_{ideal}. However, if we keep in account the ionic relaxation, other surfaces show lower W_{relaxed} values (see the third column in Tab. 1). The calculated values of the ionisation energy for the relaxed positive surface ($W^{+}_{\mathrm{relaxed}} = 6.5$ eV) and of for the relaxed negative surfaces ($W^{-}_{\mathrm{relaxed}} = 4.9$ eV) are in good agreement with the values measured by UV-photoelectron emission microscopy ($W^{+} \geq 6.2$ eV and

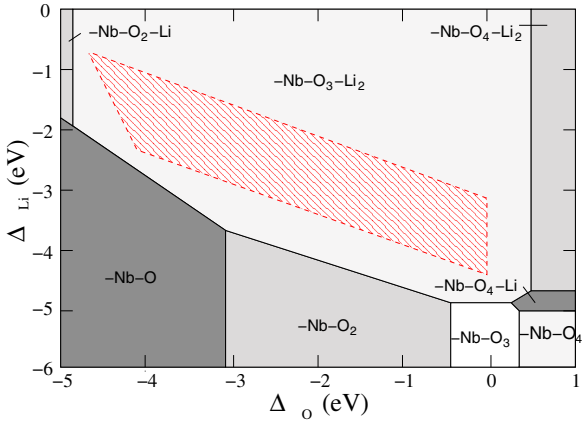

a) The positive LN (0001) surface

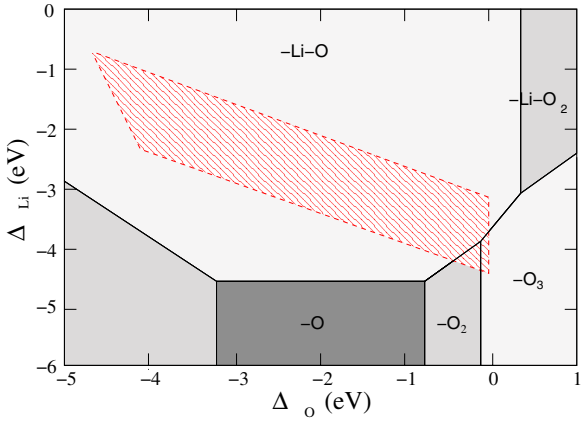

b) The negative LN (0001) surface

Figure 2 Phase diagram of the positive (a) and negative (b) LN (0001) surface. The unlabeled region corresponds to the Nb-terminated bulk cut. The highlighted region is the stability range of the LN surfaces.

$W^{-} = 4.6$ eV [7]). In the last column of Tab. 1 we report the surface dipole calculated for each termination with respect to the ideal Li terminated LN cleavage cut. This has been calculated as the variation of the potential difference from the vacuum region through the interface into the bulk. As one would expect, the stable -Nb-O_3-Li_2 termination introduces a surface dipole directed against the spontaneous polarisation, thus reducing the total polarisation. In this way the polarisation surface charge is reduced and the surface stabilised. However, other terminations would be even more effective in reducing the polarisation surface charge by introducing a surface dipole against the spontaneous polarisation, so that we have to conclude, that the preferred surface is not determined by only one dominant relaxation mechanism, but rather by the interplay of many of them. Levchenko and Rappe, whose simulations well agree with our findings, proposed recently a theoretical model to explain the stability of the preferred terminations by passivation of surface charges with ions [9].

In our investigation we have not considered other reconstructions than the 1×1. However, it is possible that reconstructions on a larger scale are stable. In fact in our simulations we only considered terminations with integer numbers of the atomic species (i.e. 0 or 1 Nb atom per unit cell), but intermediate coverages could also be stable. Nevertheless, we think that the trends we have pointed out with our simulation, like the differences in the stoichiometry of differently polarised surfaces and the propensity of the positive surface to be more oxygen rich than the negative surface, will not be affected by other possible stable terminations.

5 Conclusions We have used an *ab initio* thermodynamic approach to investigate the polar LN (0001) surfaces and gain some insight concerning the mechanisms which stabilise the preferred terminations. The phase diagrams of the positive and negative surfaces have been calculated, finding that the two surfaces under the same temperature and pressure conditions are characterised by a different stoichiometry. In general the positive surface is more oxygen rich than the negative surface. Many different stabilisation mechanisms, including surface relaxation and stoichiometry changes, are shown to contribute to the surface stability. The stable surfaces introduce a surface dipole directed against the spontaneous polarisation of the material. Finally, the calculated ionisation energy for the two surfaces differ by ≈ 1.5, showing that the ionisation energy of the LN surfaces is polarisation dependent.

Acknowledgements We thank Wolfgang Sohler and Tobias Jungk for suggesting this work and for the very helpful discussions. The calculations were done using grants of computer time from the Paderborn Center for Parallel Computing (PC^2) and the Höchstleistungs-Rechenzentrum Stuttgart. The Deutsche Forschungsgemeinschaft is acknowledged for financial support.

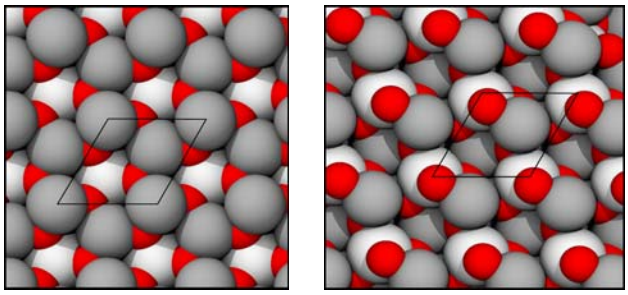

a) Positive surface b) Negative surface

Figure 3 Space-fill models of the stable positive (-Nb-O_3-Li_2 terminated) and negative (-Li-O terminated) LN (0001) surface at growth conditions. White atoms are Nb, gray atoms Li and small gray atoms O. The rhombus shows the surface unit cell.

Table 1 Ionisation energy and surface induced dipole for the investigated terminations of the positive surface. A negative dipole means that the dipol is directed against the spontaneous LN polarisation. All the values are in eV.

Termination	W_{ideal}	W_{relaxed}	$\Delta\Phi_{\mathrm{dip}}$
-Nb-O	6.9	9.7	+1.8
-Nb-O_2	10.3	9.9	+2.3
-Nb-O_3	11.1	10.3	+2.5
-Nb-O_4	10.8	8.8	+1.2
-Nb-O-Li	5.7	5.6	-2.3
-Nb-O_2-Li	5.5	5.7	-2.0
-Nb-O_3-Li	7.8	7.5	-0.1
-Nb-O_4-Li	10.1	7.6	-0.3
-Nb-O-Li_2	6.0	5.9	-1.6
-Nb-O_2-Li_2	5.6	5.5	-1.5
-Nb-O_3-Li_2	3.4	6.5	-1.4
-Nb-O_4-Li_2	9.2	10.4	+2.1

References

[1] R. S. Weis and T. K. Gaylord, Appl. Phys. A **37**, 191 (1985).
[2] G. Namkoong, K. K. Lee, S. M. Madison, W. Henderson, S. E. Ralph, and W. A. Doolittle, Appl. Phys. Lett. **87**, 171107 (2005).
[3] W. A. Doolittle, G. Namkoong, A. G. Carver, and A. S. Brown, Solid State Electron. **47**, 2143 (2003).
[4] S. Grilli, P. Ferraro, P. De Natale, B. Tiribilli, and M. Vassalli, Appl. Phys. Lett. **87**, 233106 (2005).
[5] Y. Yun and E. I. Altman, J. Am. Chem. Soc. **129**, 15684 (2007).
[6] G. H. Lee, Opt. Express **10**, 556 (2002).
[7] W.-C. Yang, B. J. Rodriguez, A. Gruverman, and R. J. Nemanich, Appl. Phys. Lett. **85**, 2316 (2004).
[8] T. Jungk, A. Hoffmann, and E. Soergel, Appl. Phys. Lett. **89**, 042901 (2006).
[9] S. V. Levchenko, and A. M. Rappe, Phys. Rev. Lett. **100**, 256101 (2008).
[10] H. Luth, Surface and Interfaces of Solids, 3rd ed. (Springer, Berlin, 1996).
[11] F. Bechstedt, Principle of Surface Physics (Springer, Berlin, 2003).
[12] D. D. Fong, A. M. Kolpak, J. A. Eastman, S. K. Streiffer, P. H. Fuoss, G. B. Stephenson, C. Thompson, D. M. Kim, K. J. Choi, C. B. Eom, I. Grinberg, and A. M. Rappe, Phys. Rev. Lett. **96**, 127601 (2006).
[13] G. Kresse and J. Furthmller, Phys. Rev. B **54**, 11169 (1996).
[14] W. G. Schmidt, M. Albrecht, S. Wippermann, S. Blankenburg, E. Rauls, F. Fuchs, C. Rödl, J. Furthmüller, and A. Hermann, Phys. Rev. B **77**, 035106 (2008).
[15] H. J. Monkhorst and J. D. Pack, Phys. Rev. B **13**, 5188 (1976).
[16] J. Neugebauer and M. Sheffler, Phys. Rev. B **46**, 16967 (1992).
[17] L. Bengtsson, Phys. Rev. B **59**, 12301 (1999).
[18] H. Xu, D. Lee, J. He, S. B. Sinnot, V. Gopalan, V. Dierolf, and S. R. Phillpot, Phys. Rev. B **78**, 174103 (2008).
[19] G. X. Qian, R. M. Martin, and D. J. Chadi, Phys. Rev. B **37**, 1303 (1988).
[20] W. G. Schmidt, B. Wenzien, and F. Bechstedt, Phys. Rev. B **49**, 4731 (1994).

